UNIVERSITY OF LEEDS

This is a repository copy of *On-line monitoring of the crystallization process: relationship between crystal size and electrical impedance spectra*.

White Rose Research Online URL for this paper:
http://eprints.whiterose.ac.uk/99361/

Version: Accepted Version

Article:

Zhao, Y, Yao, J and Wang, M (2016) On-line monitoring of the crystallization process: relationship between crystal size and electrical impedance spectra. Measurement Science and Technology, 27 (7). 074007. ISSN 0957-0233

https://doi.org/10.1088/0957-0233/27/7/074007

© 2016 IOP Publishing Ltd. This is an author produced version of a paper published in Measurement Science and Technology. Uploaded in accordance with the publisher's self-archiving policy.

Reuse
Unless indicated otherwise, fulltext items are protected by copyright with all rights reserved. The copyright exception in section 29 of the Copyright, Designs and Patents Act 1988 allows the making of a single copy solely for the purpose of non-commercial research or private study within the limits of fair dealing. The publisher or other rights-holder may allow further reproduction and re-use of this version - refer to the White Rose Research Online record for this item. Where records identify the publisher as the copyright holder, users can verify any specific terms of use on the publisher's website.

Takedown
If you consider content in White Rose Research Online to be in breach of UK law, please notify us by emailing eprints@whiterose.ac.uk including the URL of the record and the reason for the withdrawal request.

White Rose
university consortium
Universities of Leeds, Sheffield & York

eprints@whiterose.ac.uk
https://eprints.whiterose.ac.uk/

On-line Monitoring of Crystallization Process: Relationship between Crystal Size and Electrical Impedance Spectra

Yanlin Zhao[1*], Jun Yao[1,2], Mi Wang[3]

[1] Beijing Key Laboratory of Process Fluid Filtration and Separation, College of Mechanical and Transportation Engineering, China University of Petroleum-Beijing, Beijing 102249, People’s Republic of China

[2]College of Energy, Xiamen University, Xiamen 361005, People’s Republic of China

[3]Institute of Particle Science & Engineering, School of Chemical and Process Engineering, University of Leeds, Leeds LS2 9JT, United Kingdom

*Corresponding author, Email: ylzhao@cup.edu.cn

Abstract

On-line monitoring of crystal size in crystallization process is crucial to many pharmaceutical and fine-chemical industrial applications. In this paper, a novel method is proposed for on-line monitoring of the cooling crystallization process of L-glutamic acid (LGA) using electrical impedance spectroscopy (EIS). The EIS method can be used to monitor the growth of crystal particles relying on the presence of an electrical double layer on the charged particle surface and the polarization of double layer under the excitation of alternating electrical field. The electrical impedance spectra and crystal size were measured on-line simultaneously by impedance analyzer and focused beam reflectance measurement (FBRM), respectively. The impedance spectra were analyzed using the equivalent circuit model and the equivalent circuit elements in the model can be obtained by fitting the experimental data. Two equivalent circuit elements, including capacitance (C2) and resistance (R2) from the dielectric polarization of the LGA solution and crystal particle/solution interface, are related with the crystal size. The mathematical relationship between the crystal size and the equivalent circuit elements can be obtained by non-linear fitting method. The function can be used to predict the change of crystal size during the crystallization process.

Keywords: Electrical impedance spectroscopy, crystallization, particle size, on-line, equivalent circuit model

1. Introduction

Batch crystallization from aqueous solution is commonly used in the pharmaceutical and speciality fine-chemicals industries. In these industries, accurate control or monitoring of crystal size is eagerly demanded because particle size has significant effects on downstream operations such as filtration, drying, transport and storage[1-2]. Electrical impedance spectroscopy (EIS) is commonly used to investigate the dielectric properties of materials and the particle/solution interfaces[3-4]. EIS method is not a new method for measuring the particle-solution system under the static state, i.e. the properties of particles and solution do not change with time[5-7]. However, the application of EIS method for on-line monitoring of crystallization process, a dynamic process, is rarely reported in the research articles. The measurement of EIS for particle sizing ~~is~~ ~~relied~~ relies on the presence of an electrical double layer associated with the charged particle surface[8-9]. The relationship between the particle size and electrical impedance parameters has been studied in silica colloidal suspensions[10-11]. One of the advantages of the EIS method is that it can be applied in high concentration suspensions since the electrical signal is stronger from high concentration suspensions comparing optical methods. Another valuable advantage is that the EIS method has a potential to be developed into an electrical impedance tomography spectroscopy (EITS) technique [12] and hence to measure the particle size distribution in two or even three spatial dimensions with a high temporal resolution, so called dynamic imaging of particle size distribution.

Compared with the laser-based method which is commonly used for crystal size measurement[13-15], challenges in the study of crystal size by electrical impedance spectroscopy exist because the impedance data is easily affected by several factors, such as the concentration of the solid LGA phase, the concentration of solute, temperature and crystal size[16]. The relationship between the crystal size and electrical impedance spectra can’t be obtained straightforwardly, but has to rely on the establishing and solving of mathematical model.

In this paper, method of electrical impedance spectroscopy combining with equivalent circuit model was developed to get relationship between the crystal size and equivalent circuit elements. A semi-empirical equation was established to predict the change of crystal size during crystallization process from the on-line measured impedance spectra.

2. Experimental details

2.1. Experimental setup

The devices employed in our experimental set-up include a glass jacketed-vessel of three-litre capacity, a data acquisition system, an impedance analyzer (Solartron 1260), a four-electrode sensor and measurement system controller and data processing software (Smart). Temperature was controlled by a Julabo F32-HE thermostated bath. Vessel stirring was provided using a magnetic stirrer rotating at a constant speed of 400 rpm. The temperature was measured using a platinum resistance thermometer (PT100), and the turbidity was measured with a turbidimetric fiber-optic probe system built in-house. Both signals were logged onto the computer via a data acquisition system. A focused beam reflectance measurement (FBRM) device (LasenTech) was used to detect changes in particle size on-line by measuring the chord length distribution during crystallisation processes. The whole experimental setup is depicted in Figure 1. The four-electrode sensor employed in the experiments was made of stainless steel and includes two big hemispherically shaped electrodes and two needle electrodes, which have to fit the vessel.

2.2. Materials and methods

L-glutamic acid (LGA, Sigama-Aldrich Chemicals) aqueous solutions were prepared using distilled water. Electrical impedance spectra were measured by the impedance analyzer. The EIS measurement in crystallisation processes was carried out by applying an alternating excitation voltage (1 volt) with a frequency spectrum from 1 Hz to 20 MHz to the two hemispherically shaped electrodes and taking the EIS response from the two needle electrodes. The electrical impedance spectra were recorded automatically by PC during the nucleation and growth processes by the “Smart” software. The time required for testing EIS from 1Hz to ~~5~~20 MHz is about 2.5 minutes and there was no pause between loops. The four-electrode sensor which was fitted on the bottom side of the vessel’s lid was put into the jacketed vessel when it was in use. The crystallisation processes were achieved using a simple cooling method without involving any chemical reaction. The crystallization experiment was carried out in the LGA solution with the initial concentration of 21.9 g/L (saturate solution at 50 ℃). The crystallization was achieved by cooling the LGA solution from 55 ℃ to 10 ℃ at a rate of 0. 79 ℃/min and the impedance spectra at different temperatures were measured. The crystal morphologies were observed off-line by the optical microscope. The crystal sizes were measured on-line by using focused beam reflectance measurement (FBRM). FBRM measurement was started at the same time as the EIS measurement and the data were recorded by FBRM control interface software. Temperature and turbidity profiles were recorded on-line using temperature and turbidity sensors.

3. Results and discussion

In this section, on-line measured electrical impedance spectra associated with L-glutamic acid (LGA) nucleation-growth processes are presented and analysed. The relationship between the electrical impedance spectra and changing of crystal size are discussed and analysed.

3.1 Turbidity profile and crystal morphology

The crystallization process was realized by a simple cooling process and the temperature and turbidity data were recorded on-line to provide a measure of the start-point of the crystallization. Figure 2 shows the changing of turbidity with temperature associated with the LGA crystallisation process. It can be found that the transmittance data changes significantly at about 21 ℃, which indicates a fast nucleation and growth of crystals at this temperature. The crystal morphology was observed using the off-line optical microscope measurements. From the microscopic pictures (Figures 3), it can be seen that only the α-form exists during the whole crystallisation process. At the late stage of crystallisation, aggregation occurs, it can be observed that several prismatic shape crystals bind together and form a large particle with an irregular shape.

3.2 Electrical impedance spectra during the crystallization process

The electrical impedance spectra of an LGA solution (21.9 g/L) during the cooling process were recorded on-line. Figure 4 shows the electrical impedance spectra of the LGA solutions at 45.08 ℃ and 19.55 ℃, respectively. As it is known from the turbidity profile, no crystallization is occurring in solution at 45.08 ℃, but the crystals are generating and growing at 19.55 ℃. Figure 4 (a) shows two typical complex impedance plots under the conditions of crystallization and non-crystallization. Three features can be observed from the complex impedance plot: a small arc at about 1 Hz-1 kHz and a big arc at about 1 kHz-5 MHz. The small arc at low frequency range is probably due to the electrode polarization, which is coming from the electric double layer on the surface of the electrode[17]. The big arc at 1 kHz-5 MHz is a characteristic of dielectric dispersion of the solution, which includes the contribution from the polarization of charged crystals under the applied electric field and the contribution from the dielectric dispersion of medium electrolyte. It can be found that the impedance real part increases significantly when the nucleation and growth of crystals occur. Three influenced factors contribute to the increasing of real part, which are temperature, crystal particles, and the ionic concentration of solution. Figure 4 (b) shows the changes of impedance real part and imaginary part as function of frequency at 45.08 ℃ and 19.55 ℃. The peaks in the curves of impedance imaginary part represent the dielectric polarization of the LGA solution and crystal particle/solution interface. It can be observed that the relaxation frequency decreases from 1.6 MHz to 635 kHz when the crystal particles appear in the solution. The decrease of relaxation frequency is probably caused by the appearance of particle/solution interface, at where the polarization of electrical double layer occurs under the influence of the external exciting voltage[18-19]. Figure 4 (c) shows the change of impedance phase angle (θ) as function of frequency at 45.08 ℃ and 19.55 ℃. Impedance phase angle is a parameter which could characterize the dielectric properties of the materials. It can be observed that at the frequency lower than 10 kHz, the phase angles keep almost constant when temperature decreased from 45.08 ℃ to 19.55 ℃. With continuously increasing frequency from 10 kHz to 5 MHz, the absolute values of phase angle measured at 19.55 ℃, become larger than the values measured at 45.08 ℃. This phenomenon is also related with the appearance of crystal particles in the solution. The electrical double layer on the surface of crystal particle could be polarized by the exciting voltage of impedance measurement, and an induced dipole moment could be formed, which lags behind the change of applied electric field to cause a phase angle shift[10].

3.3 Equivalent circuit model and fitting results

Electrical impedance spectroscopy (EIS) data can be commonly analyzed by fitting it to an equivalent circuit model. Based on the experimental data, an equivalent circuit[20-22] was proposed and shown in Figure 5. The selection of this equivalent circuit model is based on the consideration of two dielectric relaxations which are from electrode polarization caused by the formation of ionic double layer at the interface between the solution and the electrode surfaces [22-23] and the polarization of electrical double layer on the particle surface caused by the distortion of double layer under the alternating excitation voltage [20,24]. The equivalent circuit can well fit the EIS data over the frequency range from 3 Hz to 2 MHz, based on the recognized three major EIS effects from the solution, electrode-electrolyte interface and electrolyte-particle interface. In this equivalent circuit, R_s is the ohmic resistance from solution, wire and instrument, R_1 is the resistance from the electric double layer on the electrode/solution interface, C_1 is the capacitance from the electric double layer on the electrode/solution interface[~~21~~25], R_2 is the resistance from dielectric polarization of the LGA solution and crystal particle/solution interface, C_2 is the capacitance from the dielectric polarization of LGA solution and crystal particle/solution interface.

The complex impedance of the whole system is given by:

$$Z^* = Z_s^*(R_s) + Z_1^*(R_1, C_1) + Z_2^*(R_2, C_2) \tag{1}$$

where, Z_s^* is the ohmic resistance from solution, wire, and instrument, Z_1^* is the complex impedance due to the electrode polarization occurred on the electrode/solution interface, Z_2^* is the complex impedance due to the dielectric polarization of the LGA solution and crystal particle/solution interface.

Using the resistance and capacitance in the equivalent circuit to express Z^* yields:

$$Z^* = R_e + \frac{R_1}{1+(\omega R_1 C_1)^2} - j\frac{\omega R_1^2 C_1}{1+(\omega R_1 C_1)^2} + \frac{R_2}{1+(\omega R_2 C_2)^2} - j\frac{\omega R_2^2 C_2}{1+(\omega R_2 C_2)^2} \tag{2}$$

From equation (2), separating real and imaginary parts yields

$$Z' = R_e + \frac{R_1}{1+(\omega R_1 C_1)^2} + \frac{R_2}{1+(\omega R_2 C_2)^2} \tag{3}$$

$$Z'' = -\frac{\omega R_1^2 C_1}{1+(\omega R_1 C_1)^2} - \frac{\omega R_2^2 C_2}{1+(\omega R_2 C_2)^2} \tag{4}$$

The circuit parameters (for example, R and C) can be obtained by fitting a curve to the experimental impedance data. In this study, the experimental impedance data was analyzed using “Zview” software and as an example, the fitting results for LGA solution at 19.55 ℃ are shown in Figure 6. It can be seen that the equivalent circuit model fits well with the experimental data. The fitted equivalent circuit elements during the crystallization process, including R_s, R_1, R_2, C_1 and C_2, are listed in Table 1 and also plotted as function of temperature as shown in Figure 7. It can be observed from Figure 7(a) that before the start-point of crystallization (22.5 ℃), the values of R_s, R_1 and R_2 increase slowly with decreasing temperature. However, after the start-point of crystallization, the increases of R_s, R_1 and R_2 become significant. Similar, in Figure 7(b), the values of C1 and C2 present a turning point at the start-point of crystallization. This phenomenon indicates that after the nucleation and growth of crystals, the elements of equivalent circuit become not only the functions of temperature, but also the functions of other factors, including the crystal size, solid concentration and ionic concentration. Since crystallization did not occur within the temperature range of 50℃ to 22.5℃, all of the elements of equivalent circuit (R_s, R_1, R_2, C_1, C_2) are the functions of temperature only. Based on the results in Figure 7(a), the equations of R_s, R_1 and R_2 as function of temperature can be obtained by linear fitting. The fitting results are shown in Figure 8 (a) and the equations are listed below:

$$R_s(T) = -0.157T + 24.648 \tag{5}$$

$$R_1(T) = -0.149T + 17.251 \tag{6}$$

$$R_2(T) = -2.366T + 203.339 \tag{7}$$

where, T is temperature with unit of ℃ and $22.5 \le T \le 50$℃.

The coefficients of determination for the fitting results in (5)-(7) are 0.8122, 0.9736, 0.9817, respectively.

Based on Figure 7(b), the equations of C_1 and C_2 as function of temperature can be obtained by polynomial fitting. The results are shown in Figure 8(b) and the equations are listed as following:

$$C_1(T) = 4.434\times10^{-4} + 1.090\times10^{-5}T - 7.966\times10^{-8}T^2 \tag{8}$$

$$\begin{aligned} C_2(T) = &-3.159\times10^{-8} + 5.8307\times10^{-9}T - 4.286\times10^{-10}T^2 + 1.6552\times10^{-11}T^3 \\ &- 3.542\times10^{-13}T^4 + 3.9828\times10^{-15}T^5 - 1.839\times10^{-17}T^6 \end{aligned} \tag{9}$$

where, T is temperature with unit of ℃ and $22.5 \le T \le 50$℃.

The coefficients of determination for the fitting results in (8)-(9) are 0.8250 and 0.8987, respectively.

In the temperature range of 22.5℃ to 10℃, the situation becomes complicated due to the occurrence of crystallization. Since R_1 and C_1 are related ~~with~~ to the electric double layer on the electrode/solution interface, they should be functions of ionic concentration in the solution. R_s is the ohmic resistance from solution, wire and instrument, therefore it should be a function of ionic concentration as well. The equivalent circuit elements R_1, C_1 and R_s are crystal size independent. Equivalent circuit elements R_2 and C_2 represent the dielectric polarization from LGA solution and particle/solution interface; therefore it is a function of crystal size. As shown in Fig (7), R and C have different slope against temperature after 22.5 ℃, compared with temperature before 22.5 ℃. The reason is that before 22.5 ℃ (the nucleation point), the equivalent circuit elements are only affected by the temperature, whereas after 22.5 ℃, the equivalent circuit are affected not only by the temperature, but also by the crystals and ionic concentration in the solution. ~~Because~~ Since the cooling rate was kept constant at the temperature range of 50 ℃ -10 ℃, the changing rate of temperature during EIS measurement is same. Therefore, the changes of equivalent circuit elements caused by changing temperature before and after nucleation could be treated same. ~~the temperature effect on the equivalent circuit elements during nucleation and growth of crystals could be treated as same as the stage before nucleation.~~ The equations (5)–(9) represent the temperature dependence of equivalent circuit elements, which do not include other effects from crystals and ionic solution. Therefore, equations (5)–(9) should hold up at the range of 50℃ -10℃.T~~he equations (5)-(9) can hold up at the range of 50 ℃ -10 ℃ .~~

3.4 Relationship between crystal size and equivalent circuit elements

In this section, the relationship between crystal size and equivalent circuit elements, R_2, C_2, is analysed and a semi-empirical equation based on the experimental data is developed. The chord length of the crystal particle during crystallisation process was recorded on-line using FBRM method[~~22~~26]. Although the chord length given by FBRM measurement is not the real diameter of crystal, it is treated as equivalent crystal size in this study. The changes of mean chord length (a) of crystal particles, R_2 and C_2 with temperature are shown in Figure 9. From Figure 9, it can be found that the mean chord length of crystal particles increases significantly with decreasing temperature. Since the dielectric polarization of the crystal particle/solution interface is related with electrical double layer on the particle surface and the diffusion of ions along the surface, the size of the crystal particle plays an important role on dielectric polarization. Thus, the crystal size is the function of the equivalent circuit elements of R_2 and C_2. In order to get the relationship between the crystal size and R_2, C_2, the temperature effect on the equivalent circuit elements after nucleation need to be eliminated. For the cooling process with a constant cooling rate, the temperature effect on R_2 and C_2 before nucleation and after the nucleation can be treated as the same. With the assumption, the temperature effect represented by equations (5)-(9) can be extended over the range of 50 ℃ -10 ℃, which provides an opportunity to separate and remove the temperature effect on EIS data during the cooling period of nucleation. The temperature effect can be removed by subtracting the contribution of temperature on R_2 and C_2 using equations (7) and (9). The temperature contribution on R_2 and C_2 (denoted by $R_{2,T}$ and $C_{2,T}$) can be calculated using equations (7) and (9) at the temperature range of 22.77 ℃ -13.13 ℃ . $R_{2,T}$ and $C_{2,T}$ are smaller than R_2 and C_2 (shown in the Table 1), since they do not include other influences except for the temperature. Therefore, ~~The~~ the equivalent circuit elements of R_2' and C_2' after correction of temperature effect can be calculated by equation (10) and (11) and the results are listed in Table 2.

$$R_2' = R_2 - R_{2,T} \qquad (10)$$

Field Code Changed

$$C_2' = C_2 - C_{2,T} \qquad (11)$$

Field Code Changed

Now the crystal size (a) is the function of R_2' and C_2' as shown by:

$$a = f(R_2', C_2') \qquad (\cancel{10}12)$$

The form of equation can be obtained by non-linear fitting the experimental data to get a smallest root of mean square error. The result is shown by the equation (~~11~~13):

$$\begin{aligned} a = {} & p1 + p2\times R_2' + p3\times R_2'^2 + p4\times R_2'^3 + p5\times R_2'^4 + p6\times R_2'^5 \\ & + p7\times \ln C_2' + p8\times(\ln C_2')^2 + p9\times(\ln C_2')^3 + p10\times(\ln C_2')^4 \end{aligned} \qquad (13\cancel{11})$$

where , p1-p10 are the constants and shown in the below:

$$p1 = -102449.786$$
$$p2 = 1.5246$$
$$p3 = -0.004586$$
$$p4 = -0.0001114$$
$$p5 = 6.16 \times 10^{-7}$$
$$p6 = -6.12 \times 10^{-10}$$
$$p7 = -17746.3663$$
$$p8 = -1143.6664$$
$$p9 = -32.5396$$
$$p10 = -0.34517$$

The calculated crystal size using equation (~~11~~13) and the measured crystal size by FBRM are show in the table 3. It can be found that the calculated crystal size is close to the measurement results by FBRM. ~~The equation (11) can be used to predict the crystal size during the crystallization process.~~ The equation (~~11~~13) provides an empirical approach to predict the crystal size during the LGA crystallization process.

4. Conclusions

The electrical impedance spectroscopy method was used for on-line monitoring of the crystallization process of L-glutamic acid. An equivalent circuit model was proposed to analyze the electrical impedance spectra. The equivalent circuit elements were obtained by fitting the experimental data in to the equivalent circuit model. Within the temperature range of 50℃ to 22.5℃, all of the equivalent circuit elements are the function of temperature only, since the crystallization did not occur. Therefore, the equations of R_s, R_1 and R_2 as function of temperature were obtained by linear fitting and the equations of C_1 and C_2 as function of temperature were obtained by polynomial fitting. When the temperature is lower than 22.5 ℃, the nucleation and growth of crystal particles occurred. In the equivalent circuit model, the resistance (R_2) and capacitance (C_2) from the dielectric polarization of the LGA solution and crystal particle/solution interface are not only related with temperature, but also related to the crystal size. After eliminating the temperature effect, the crystal size is the function of equivalent circuit elements of $R_2^{'}$ and $C_2^{'}$. A semi-empirical equation which could be used to describe the relationship between the crystal size and equivalent circuit elements of $R_2^{'}$ and $C_2^{'}$, has been developed by non-linear fitting method. The equation could be used to predict the changing of crystal size during the crystallization process. The EIS with the proposed methods of the equivalent circuit, temperature effect correction and non-linear fitting computation could be used to predict the changing of crystal size for general crystallization process with particular attentions on the conditions of a constant cooling rate required in the elimination of temperature effect and recalculation of fitting constants in the empirical equation normally necessary.

Acknowledgements

This work was supported by National Natural Science Foundation of China (No. 51406235; 51376153); Science foundation of China University of Petroleum, Beijing (No. 2462013YJRC030, 2462015YQ0402).

References

[1] Alatalo H, Hatakka H, Kohonen J, Reinikainen S and Louhi-kultanen M 2010 Process control and monitoring of reactive crystallization of L-glutamic acid AIChE Journal, 56, 2063-2067.

[2] Schorsch S, Vetter T and Mazzotti M 2012 Measuring multidimensional particle size distributions during crystallization Chem Eng Sci, 77, 130-142.

[3] Macdonald J R 1987 Impedance spectroscopy, emphasizing solid materials and systems A Wiley-Interscience publication.

[4] Bradshaw-Hajek B H, Miklavcic S J and White L R 2010 The actual dielectric response function for a colloidal suspension of spherical particles Langmuir, 26, 7875-7884.

[5] Grosse C and Delgado A V 2010 Dielectric dispersion in aqueous colloidal systems Curr. Opin. Colloid Interface Sci. 15, 145-159.

[6] Delgado A V, Arroyo F J, Gonzalez-Caballero F, Shilov V N and Borkovskaya Y B 1998 The effect of the concentration of dispersed particles on the mechanisms of low-frequency dielectric dispersion (lfdd) in colloidal suspensions 1998 Colloids Surf. A, 140, 139-149.

[7] Delacey E H B and White L R 1981 Dielectric response and conductivity of dilute suspensions of colloidal particles J. Chem. Soc., Faraday Trans, 77, 2007-2039.

[8] Arroyo F J, Carrique F, Bellini T and Delgado A V 1999 Dielectric dispersion of colloidal suspensions in the presence of stern layer conductance: Particle size effects J. Colloid Interface Sci. 210, 194-199.

[9] Carrique F, Arroyo F J and Delgado A V 1998 Effect of size polydispersity on the dielectric relaxation of colloidal suspensions: A numerical study in the frequency and time domains J. Colloid Interface Sci. 206, 569-576.

[10] Zhao Y and Wang M 2015 Experimental Study on Dielectric Relaxation of SiO2 Nano-particle Suspensions for Developing a Particle Characterization Method based on Electrical Impedance Spectroscopy Powder Technology 281, 200-213.

[11] Zhao Y, Wang M and Hammond R B 2013 Characterisation of Nano-particles: Relationship between Particle Size and Electrical Impedance Spectra J Nanosci Nanotechno 13(2), 808-812.

[12] Nahvi M and Hoyle B S 2008 Wideband electrical impedance tomography Meas. Sci. Technol. 19, 094011-1-9.

[13] Abbas A, Nobbs D and Romagnoli J 2002 A Investigation of on-line optical particle characterization in reaction and cooling crystallization systems. Current state of the art, Meas. Sci. Technol. 3, 349–356.

[14] Scholl J, Bonalumi D, Vicum L, Mazzotti M and Muller M 2006 In situ monitoring and modeling of the solvent-mediated polymorphic transformation of l-glutamic acid", Cryst. Growth Des. 6, 881-891.

[15] De Anda J C, Wang X Z, Lai X, Roberts K J, Jennings K H, Wilkinson M J, Watson D and Roberts D 2005 Real-time product morphology monitoring in crystallization using imaging technique", AIChE Journal, 51, 1406-1414.

[16] Zhao Y, Wang M and Hammond R B 2011 Characterisation of Crystallisation Processes with Electrical Impedance Spectroscopy Nucl. Eng. Des. 241, 1938-1944.

[17] Asami K 2011 Design of a measurement cell for low-frequency dielectric spectroscopy of biological cell suspensions Meas. Sci. Technol. 22(8) 85801-85807(7).

[18] Dukhin S S and Shilov V N 1980 Kinetic aspects of electrochemistry of disperse systems.2.Induced dipole-moment and the nonequilibrium double-layer of a colloid particle Adv. Colloid Interface Sci. 13, 153–195.

[19] O'Brien R W 1982 The response of a colloidal suspension to an alternating electric-field Adv. Colloid Interface Sci. 16, 281–320.

[20] Dudley L M, Bialkowski S, Or D and Junkermeier C 2003 Low frequency impedance behaviour of montmorillonite suspensions: Polarization mechanisms in the low frequency domain, Soil Sci. Soc. Am. J. 67, 518–526.

[21] Blewett J, McCarter W J, Chrisp T M, Starrs G 2001 Monitoring sedimentation of a clay slurry Géotechnique 51, No.8, 723-728.

[22] Franks W, Schenker I, Schmutz P and Hierlemann A 2005 Impedance characterization and modeling of electrodes for biomedical applications IEEE Trans. Biomed. Eng. 52 1295–302.

[23] Bechi M, Avendano C, Strigazzi A, Barbero G 2005 Impedance spectroscopy of water solutions: the role of ions at the liquid-electrode interface J. Phys. Chem. B 109, 23444-23449.

[24] Roldán-Toro R and Solier J D 2004 Wide-frequency-range dielectric response of polystyrene latex dispersions J. Colloid Interface Sci. 274, 76-88.

[~~21~~25] Ben Ishai P, Talary M S and Caduff A 2013 Electrode polarization in dielectric measurements: a review Meas. Sci. Technol. 24, 102001-1-21.

[~~22~~26] Agimelen O S, Hamilton P and Haley L 2015 Estimation of particle size distribution and aspect ratio of non-spherical particles from chord length distribution Chem Eng Sci 123, 629-640.

Tables:

Table 1: The fitted equivalent circuit elements during the crystallization process, including R_s, R_1, R_2, C_1 and C_2

Temperature (°C)	R_s (ohm)	R_1 (ohm)	C_1 (F)	R_2 (ohm)	C_2 (F)
50.7	16.9	9.975	7.866E-4	87.89	1.01E-09
45.08	17.57	10.59	7.7793E-4	96.78	1.00E-09
39.9	18.73	11.12	7.524E-4	106.3	9.91E-10
36.47	19.35	11.48	7.472E-4	113.7	9.90E-10
32.84	17.95	12.17	7.1689E-4	124.4	9.89E-10
31.17	19.53	12.54	6.8529E-4	127.4	9.79E-10
29.49	19.85	12.7	7.1462E-4	132.3	9.79E-10
27.8	20.17	13.15	6.5504E-4	137.3	9.79E-10
24.45	20.89	13.76	6.7961E-4	148.5	9.79E-10
22.77	21.96	14.13	5.9236E-4	152.9	1.02E-09
21.8	22.15	14.7	5.6615E-4	157	1.02E-09
21.38	22.35	13.54	8.0445E-4	164	1.01E-09
21.08	23.54	12.45	0.00123	180.6	9.76E-10
20.39	25.33	12.89	0.00146	204.6	9.39E-10
19.55	27.66	14.81	0.00126	229.8	9.24E-10
18.47	28.47	16.42	0.001	254.9	9.14E-10
17.23	30.04	17.79	8.7369E-4	277.2	8.94E-10
15.92	31.84	18.88	8.3202E-4	300.1	8.87E-10
14.51	32.59	19.81	7.714E-4	322.8	8.76E-10
13.13	34.68	22.17	6.7728E-4	344.5	9.26E-10

Table 2 The equivalent circuit elements of $R_2^{'}$ and $C_2^{'}$ after correction of temperature effect.

Temperature (°C)	$R_2^{'}$ (ohm)	$C_2^{'}$ (F)
22.77	3.43482	4.9381E-11
21.8	5.2398	5.99271E-11
21.38	11.24608	6.09081E-11
21.08	27.13628	3.55654E-11
20.39	49.50374	2.20859E-11
19.55	72.7163	4.885E-11
18.47	95.26102	1.19497E-10
17.23	114.62718	2.43112E-10
15.92	134.42772	4.70729E-10
14.51	153.79166	8.44308E-10
13.13	172.22658	1.44745E-09

Table 3 Comparison of measured crystal size (FBRM) and calculated crystal size

Temperature (°C)	Measured crystal size a (μm)	Calculated crystal size a (μm)
22.77	26.502	26.378
21.8	31.179	31.472
21.38	40.518	40.273
21.08	54.186	54.285
20.39	70.336	70.350
19.55	81.007	80.833
18.47	89.017	89.407
17.23	96.045	95.567
15.92	99.258	99.599
14.51	101.984	101.840
13.13	104.970	104.997

Figure1

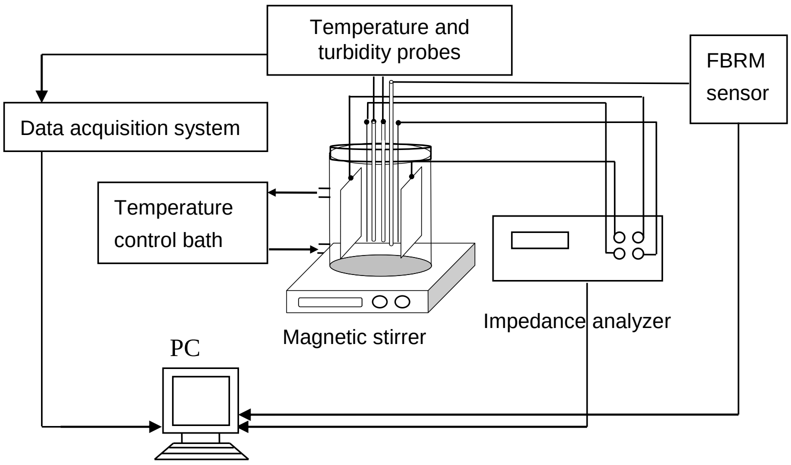

Figure 1: Experimental setup

Figure 2

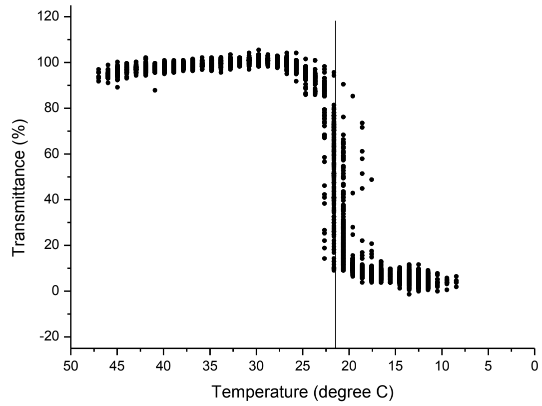

Figure 2: Turbidity data obtained during the crystallization of LGA (21.9 g/L) at a cooling rate of 0.79 ℃/min from 55℃ to 10℃.

Figure 3

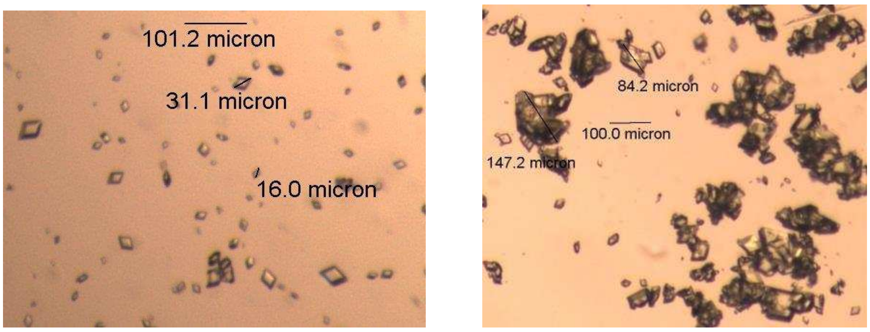

(a) at 20 ℃

(b) at 10 ℃

Figure 3: Crystal morphology at the early stage (a) and late stage (b) of crystallisation.

Figure 4

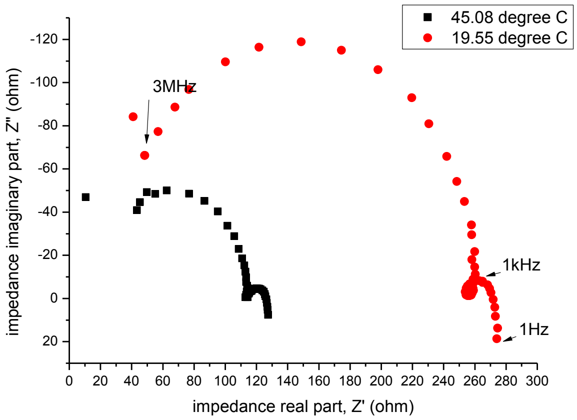
45.08 degree C
19.55 degree C
3MHz
1kHz
1Hz
-120
-100
-80
-60
-40
-20
0
20
impedance imaginary part, Z'' (ohm)
0
20
40
60
80
100
120
140
160
180
200
220
240
260
280
300
impedance real part, Z' (ohm)

(a)

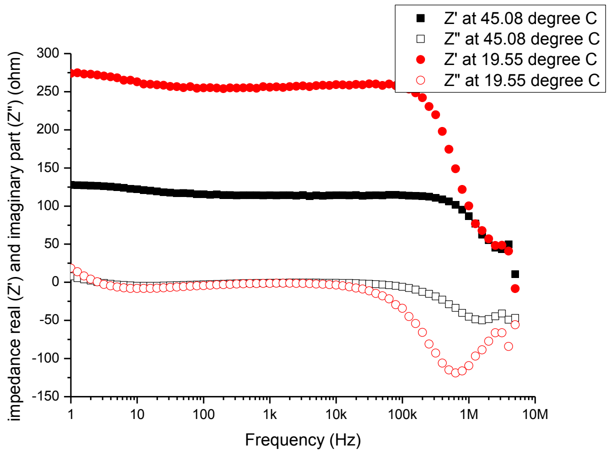
Z' at 45.08 degree C
Z'' at 45.08 degree C
Z' at 19.55 degree C
Z'' at 19.55 degree C
300
250
200
150
100
50
0
-50
-100
-150
impedance real (Z') and imaginary part (Z'') (ohm)
1
10
100
1k
10k
100k
1M
10M
Frequency (Hz)

(b)

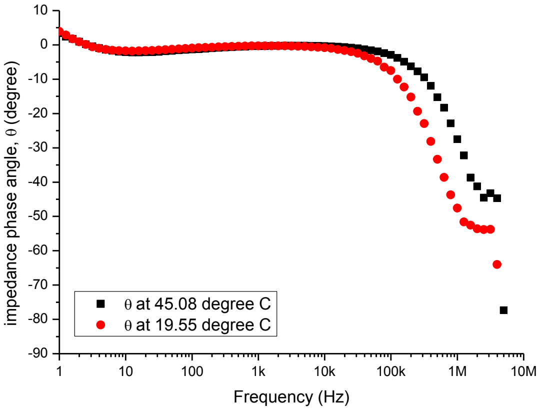

(c)

Figure 4: (a) complex impedance plot; (b) impedance real part and imaginary part vs. frequency plots (c) impedance phase ange vs. frequency plots at 45.08 ℃ and 19.55 ℃, respectively.

Figure 5

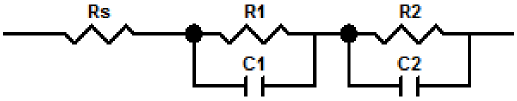

Figure 5: Equivalent circuit model for EIS data

Figure 6

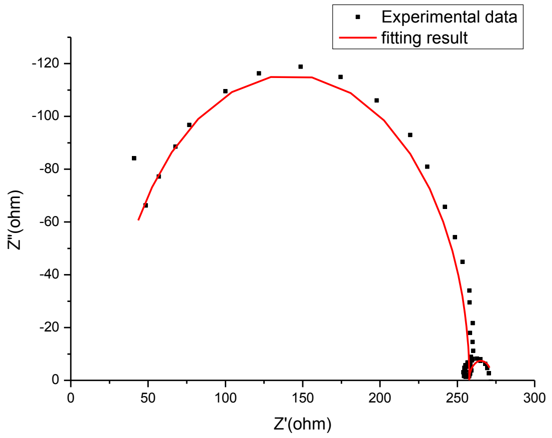

(a)

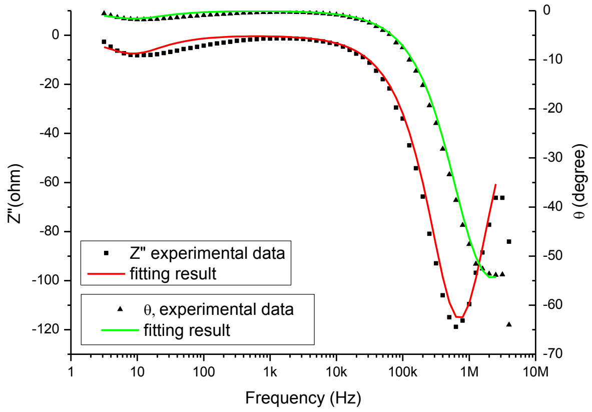

(b)

Figure 6: The experimental data and fitting result for crystal suspension at 19.55 ℃ using equivalent circuit: (a) complex impedance plot; (b) impedance parameters vs. frequency plots.

Figure 7

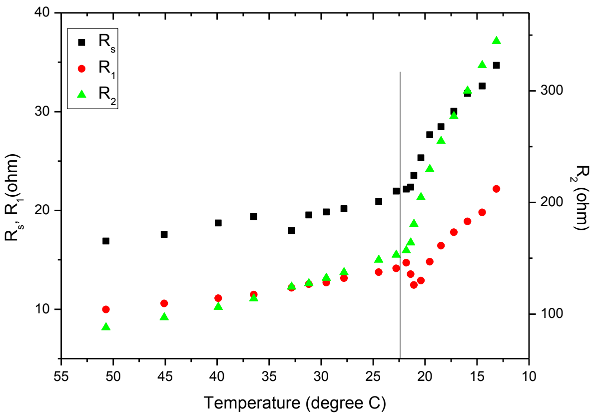

(a)

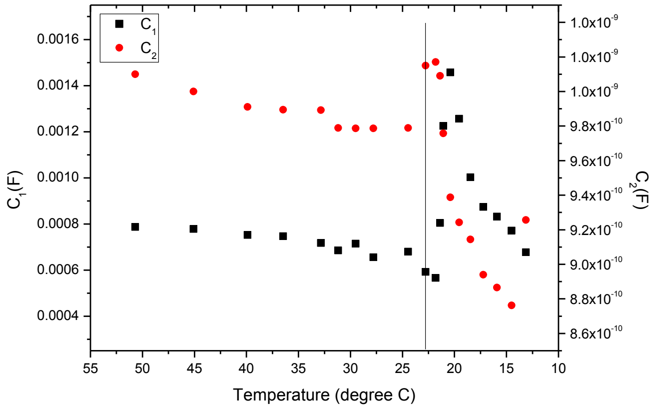

(b)

Figure 7: Elements of equivalent circuit to fit the impedance data: (a) R_s, R_1 and R_2 change as function of temperature during the crystallization process; (b) C_1 and C_2 change as function of temperature during the crystallization process.

Figure 8

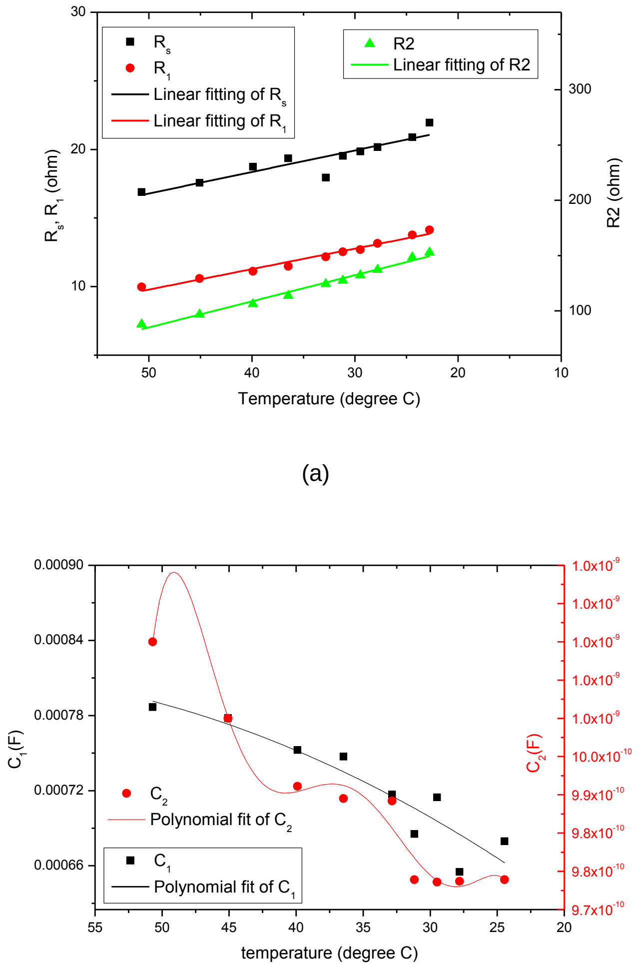

(a)

(b)

Figure 8: Fitting results for equivalent circuit elements as function of temperature before crystallization (a) R$_s$, R$_1$ and R$_2$; (b) C$_1$, C$_2$.

Figure 9

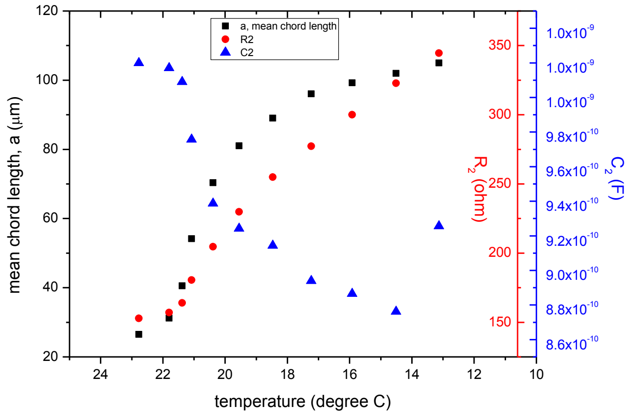

Figure 9: The changes of mean chord length of crystal particles, R_2 and C_2 during the crystallization process

Figure Captions

Figure 1: Experimental setup

Figure 2: Turbidity data obtained during the crystallization of LGA (21.9 g/L) at a cooling rate of 0.79 ℃/min from 55℃ to 10℃.

Figure 3: Crystal morphology at the early stage (a) and late stage (b) of crystallisation.

Figure 4: (a) complex impedance plot; (b) impedance real part and imaginary part vs. frequency plots (c) impedance phase ange vs. frequency plots at 45.08 ℃ and 19.55 ℃, respectively.

Figure 5: Equivalent circuit model for EIS data.

Figure 6: The experimental data and fitting result for crystal suspension at 19.55 ℃ using equivalent circuit: (a) complex impedance plot; (b) impedance parameters vs. frequency plots.

Figure 7: Elements of equivalent circuit to fit the impedance data: (a) Rs, R1 and R2 change as function of temperature during the crystallization process; (b) C1 and C2 change as function of temperature during the crystallization process.

Figure 8: Fitting results for equivalent circuit elements as function of temperature before crystallization (a) Rs, R1 and R2; (b) C1, C2.

Figure 9: The changes of mean chord length of crystal particles, R2 and C2 during the crystallization process